J Mater Sci: Mater Electron (2008) 19:406–410
DOI 10.1007/s10854-007-9354-x

Effect of underfill on bending fatigue behavior of chip scale package

Bo-In Noh · Noh-Chang Park · Won-Sik Hong · Seung-Boo Jung

Received: 21 March 2007 / Accepted: 15 June 2007 / Published online: 10 July 2007

Abstract This study evaluated the mechanical behavior of chip scale packages (CSPs) with the underfills using the four-point bending test. The bending fatigue durability in the CSP increased with increasing glass transition temperature (T_g) of the underfill. The mechanical fatigue cracks occurred in the region between the $(Ni,Cu)_3Sn_4$ layer and the solder region near the upper substrate and the solder region of the CSP with the underfill which had the higher T_g. However, these cracks occurred in the region between the $(Ni,Cu)_3Sn_4$ layer and the Ni_3P layer near the bottom substrate and the solder region of the CSP with the underfill which had the lower T_g.

1 Introduction

The development of integrated circuit (IC) packaging has stressed the need for a smaller, thinner, lighter and higher density package configuration [1]. Therefore, the ball pitch becomes finer, while both the pad and ball are reduced in size. Ball grid array (BGA) packages and chip scale packages (CSPs) are now widely used for many electronic applications, including portable and telecommunication products [2–5]. The CSPs provide excellent electrical performance, high input/output (I/O) density and interconnection speed, and good manufacturability with high reliability [6, 7]. The reliability of CSPs in portable devices is questionable due to the mechanical stresses experienced during their service lifetime. These stresses are primarily generated due to impact, shock, vibration, mechanical bending, and thermally-induced fatigue due to coefficient of thermal expansion (CTE) mismatch between the CSPs and printed circuit board (PCB).

The underfill process dispenses the non-conductive epoxy between the chip and the substrate around the chip interconnection. When the underfill is cured, the underfill can serve the multiple functions. Underfill reduces the package stresses caused by the CTE mismatch between the silicon, solder alloy, and organic substrate. Underfill reduces the shear strain of the device and the PCB, protects the chip from the external environment, provides mechanical strength to the whole package, and thereby greatly improves the solder joint reliability and package service life [3, 8, 9].

The board level reliability of fine pitch package has been investigated by bending test, thermal cycle test, tensile test and metallurgical characterization [10–12]. The routine applications of portable electronic devices induce low-frequency, random vibration to the electronic packages within. Owing to the increasing demand of these devices, the reliability of electronic packages subjected to repetitive mechanical loads has become an important issue in the contemporary electronic packaging industry. For cyclic bending reliability in particular, studies have been carried out for specific packages under different test conditions at the board- or system-level [10–12]. The four-point bending test is widely used because it is suitable for testing large package sample under similar loading conditions (bending

B.-I. Noh · S.-B. Jung (✉)
School of Advanced Materials Science and Engineering, Sungkyunkwan University, 300 Cheoncheon-dong, Jangan-gu, Suwon 440-746, Republic of Korea
e-mail: sbjung@skku.ac.kr

N.-C. Park · W.-S. Hong
Reliability & Failure Analysis Center, Korea Electronics Technology Institute, 68 Yatap-dong, Bundang-gu, Seongnam 463-816, Republic of Korea

moments) within the inner load span. The bending fatigue response of a solder joint is a multi-variant process depending on several parameters such as PCB thickness and its elastic modulus, solder joint size, array configuration, pad size, span (distance from package to support points), amount of localized pressure imparted to the package and PCB, mechanical stiffness of the package and temperature [10–12].

Many studies have investigated the reliability of CSPs under the conditions imposed by accelerated tests [10–12], but few have examined the reliability of CSPs with the various underfills under mechanical condition. Therefore, in this study, the effect of underfill on bending fatigue behavior of CSPs was evaluated using four-point bending test.

2 Experimental procedure

The solder balls used in this experiment had a diameter of 300 μm and composition of Sn–3.0 wt%Ag–0.5 wt%Cu. The chip dimensions were 9.0 mm × 9.0 mm with 96 I/Os. The upper substrate was primarily made of polyimide and the surface finish on the upper substrate consisted of an electrolytic Au/Ni on a Cu pad. The dimensions of the flame resistant-4 (FR-4) bottom substrate were 100 mm × 50 mm × 1.0 mm. The opening size of the pad was 280 μm with a pitch of 500 μm. The surface finish on the FR-4 substrate consisted of an electroless Ni-P/immersion Au (ENIG) on a Cu pad. The Ni-P layer of the FR-4 substrate had an amorphous structure containing 15 at.%P.

The reflow temperature was 245 °C, and the flux residues were removed after the reflow soldering process. After the flux residues were removed, the underfill was dispensed to the samples which were then cured in an oven for 40 min at 125 °C. The three kinds of underfill were made in this study. The proportions of epoxy resin, hardener, diluent and appendix were 60.0, 25.0, 10.0 and 5.0%, respectively. Instead of the same proportions, underfills A, B and C were composed of the bisphenol-A-type epoxy resin, a mixture of epoxy resins of bisphenol-A-type and novolac-type, and the novolac-type epoxy resin, respectively.

To measure the glass transition temperature (T_g) of the underfills, differential scanning calorimetry (DSC) was carried out. The DSC was conducted from 25 to 250 °C at a heating rate of 5 °C/min in a nitrogen atmosphere.

After the underfill was cured, the CSPs were subjected to four-point bending test. The tip of each support was a roller to ensure a line contact with the test board. The bottom supports were fixed, while the top supports move downwards repetitively with the displacement profile prescribed by the sinusoidal movement of the actuator. The top and bottom spans were fixed at 30 mm and 80 mm, apart. The solder interconnects of each test unit were daisy-chained and an event detector was utilized to record the overall electrical resistance of each specimen in-situ. The applied current of the package was 0.01 A. The event detector was triggered whenever the overall electrical resistance exceeded 150 Ω. The experiments were performed at room temperature. We conduct the test under the condition of a combined applied force of 25.4 N, which was 10% of the maximum strength of test unit, and an excitation frequency of 1 Hz. The maximum strength of test unit was measured using the three-point bending test. The three-point bending test was conducted with an applied force of 50 kgf at a speed of 10 mm/min. The maximum strength was defined as an open circuit within the test unit.

After the four-point bending test, the samples were mounted in epoxy, cross-sectioned, ground, and polished for microstructural observation. In order to examine the intermetallic compounds (IMCs) and fatigue failure mode during the four-point bending test, the cross-sections of all specimens were observed with scanning electron microscope (SEM). The intermetallic phase was identified with energy dispersive spectrometry (EDS).

3 Results and discussions

Figure 1 shows the non-isothermal DSC results of the underfills. Full curing with lower curing temperature and longer curing time of the underfill is known to lead to lower thermal stress and better physical and mechanical properties. From these results, it was identified that the T_g of underfill A was the lowest while that of underfill C was the highest. It was estimated that the novolac-type epoxy resin has the many reactors and a high cross-linking degree

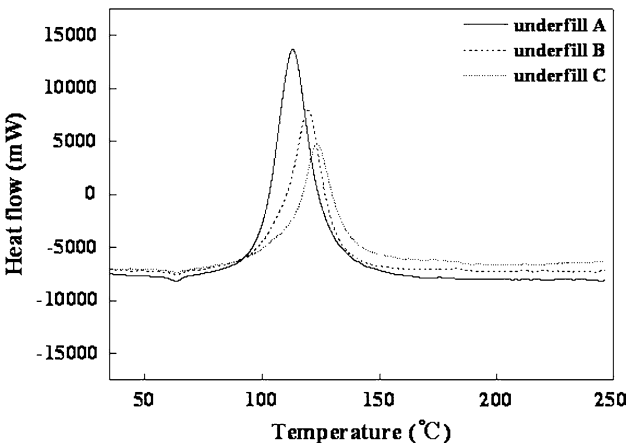

Fig. 1 Results of DSC for underfills

which led to the increased in T_g. Therefore, underfill C was considered to be more suitable because the highest T_g of underfill C indicates greater rigidity, thereby reducing the mechanical stresses during bending test.

Figure 2 shows the variations of force and voltage of package with various underfills under four-point bending test. The material properties of the package, substrate, and PCB combined to detract from the bending fatigue reliability. When the load was pressed into the PCB under the bending test, the PCB was warped and the solder joints failed. As the uniform package current was applied under bending test, the voltage change of package was equivalent to the electrical resistance change of the package. When a crack or failure occurred in the package, the force change of the package and electrical resistance change of the package were excessive. When the packages with and without underfill were compared, the fatigue life of the former was longer than that of the latter, indicating that the cured underfill of the package had absorbed the warpage of the package and propagated the solder cracks. In the case of the package without underfill, the fatigue life was about 780 cycles, compared to about 890, 4,790 and 30,500 cycles for the packages with underfills A, B and C, respectively. These results confirmed that the packages with underfill C had the highest bending fatigue resistance, and the high bending fatigue resistance of the package with underfill C was due to its high T_g. In addition, the strong chain-linking of the underfill supported a good absorption property for bending fatigue deformation. Underfill A, however, which was composed of the bisphenol-A-type epoxy resin had the lowest bending fatigue resistance. Therefore, it was estimated that the properties and presence or absence of underfill were affected by the bending fatigue resistance of package.

Figure 3 shows the images representing the crack propagation path in CSPs after the four-point bending test. The EDS analysis showed that the composition of the IMCs formed at the interface between solder and substrate was 28.0at.% Ni, 16.0at.% Cu, and 56.0at.%Sn, which indicated a $(Ni,Cu)_3Sn_4$ phase. A Ni_3P layer was formed at the bottom interface between $(Ni,Cu)_3Sn_4$ and electroless Ni-P layer. The Ag_3Sn phases were dispersed within the matrix. We identified that the bending fatigue crack of the solder initiated from the corner joint and propagated towards the inner joint of the package. When the load was pressed into the PCB under the four-point bending test, the PCB was warped and the solder joints failed. According to previous studies [13, 14], the solder joints located at the outermost row suffered the most deformation applied, while the central joint experienced only minimum stress due to the difference in bending rigidity of the package and PCB. In addition, the crack occurred via two modes in the

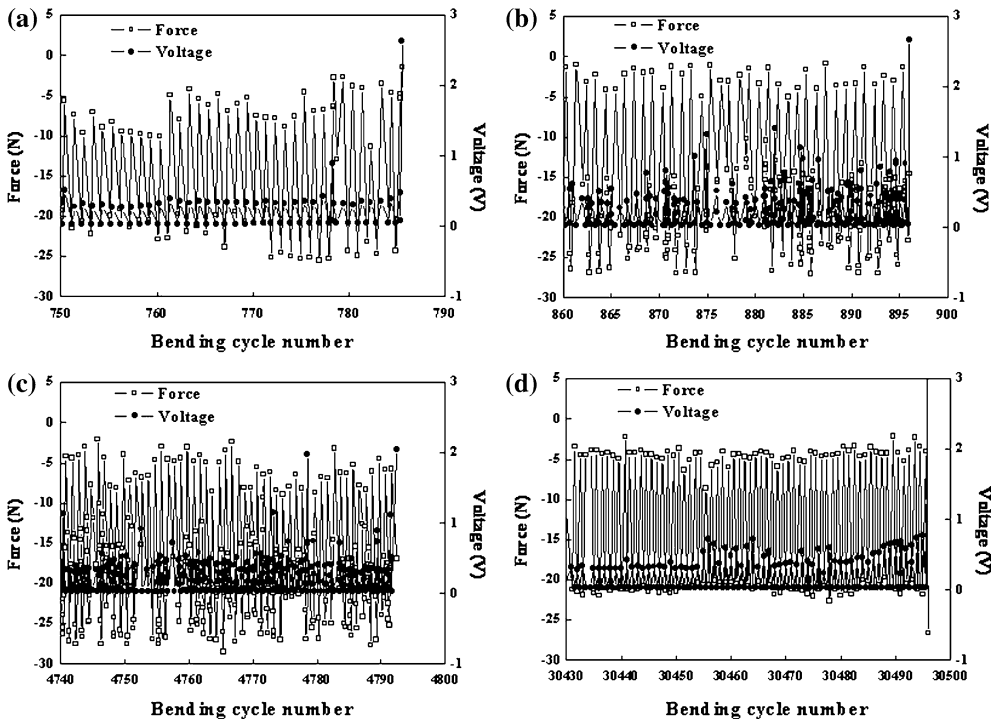

Fig. 2 Variations of force and voltage of package with various underfills under bending test: (**a**) no-underfill, (**b**) underfill A, (**c**) underfill B and (**d**) underfill C

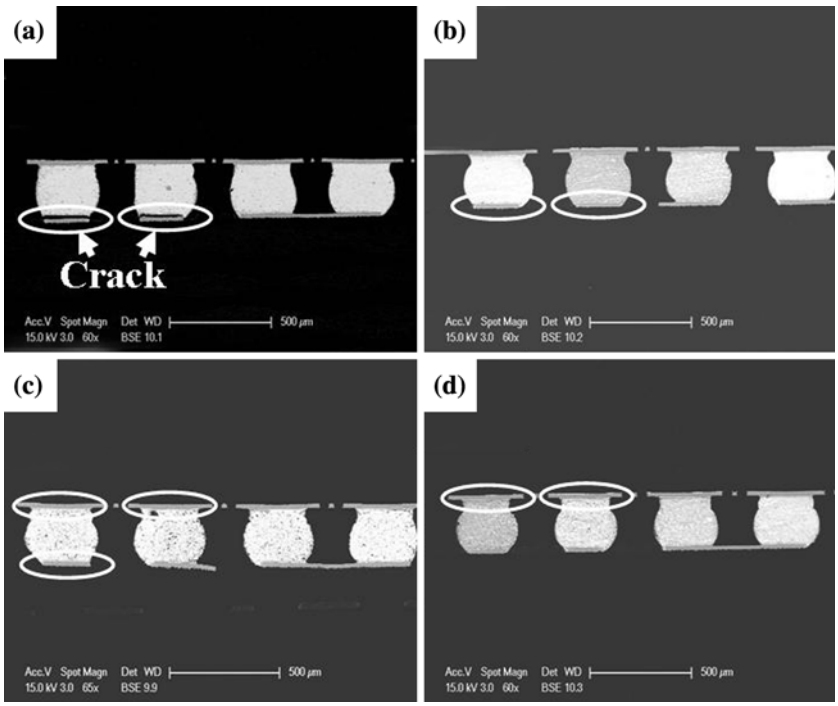

Fig. 3 Cross sectional SEM images of CSPs after the bending test: (**a**) no-underfill, (**b**) underfill A, (**c**) underfill B and (**d**) underfill C

package: one in the region between the upper substrate and the solder region for the package with higher bending fatigue resistance, and the other between the IMCs of the bottom substrate and the Ni_3P layer for the package with lower bending fatigue resistance. Also, the fatigue mode of package without underfill was the latter.

Figure 4 shows the cross sectional SEM images of CSPs with various underfills after the four-point bending test. An important deformation characteristic of solder balls under bending condition is that the joint is under a biaxial and tension-dominated stress state, rather than a shear-dominated deformation mode. When the packages with and without underfill were compared, the latter had a larger width and crack length. In addition, the package with underfill C had a smaller width and crack length than that with underfills A and B, indicating that underfill C had

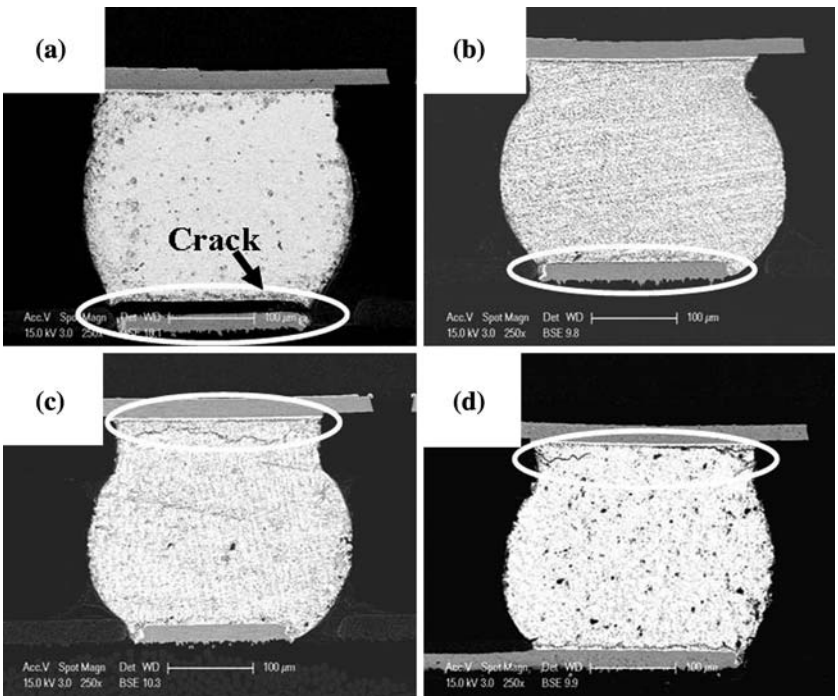

Fig. 4 Cross sectional SEM images of CSPs with various underfills after the bending test: (**a**) no-underfill, (**b**) underfill A, (**c**) underfill B and (**d**) underfill C

better resistance to the bending fatigue failure because of its higher T_g. Furthermore, the package crack occurred in different regions, according to the bending fatigue resistance of the package. The crack occurred in the region between the upper substrate and the solder region for the package with higher bending fatigue resistance, but in the region between the IMCs of the bottom substrate and the Ni_3P layer for the package with lower bending fatigue resistance. Therefore, the package stiffness plays an important role and as the material selection affects the package and underfill stiffness, it directly influences the interconnect reliability when the package is subjected to mechanical bending fatigue behavior.

4 Conclusions

The properties and presence or absence of underfill were affected by the CSPs bending behavior. The cured underfill of the package absorbed the package warpage and propagated the solder crack under bending conditions. Because the novolac-type epoxy resin had reinforced underfill cross-linking, the underfill which was composed the novolac-type epoxy resin had the higher resistance for bending fatigue than that of the underfill which was composed the bisphenol-A-type epoxy resin. The mechanical fatigue cracks occurred in the region either between the upper substrate and the solder region or between the bottom substrate and the solder region of the CSP with the underfill which had the higher or lower T_g, respectively.

Acknowledgements This work was supported by grant No. RTI04–03-04 from the Regional Technology Innovation Program of the Ministry of Commerce, Industry and Energy (MOCIE).

References

1. U.D. Perera, Microelectron. Reliab. **39**, 391 (1999)
2. R. Ghaffarian, Microelectron. Reliab. **43**, 695 (2003)
3. J.H. Lau, *Flip Chip Technologies*. (McGraw-Hill, New York, 1996), pp. 123–153
4. R. Daveaux, J. Heckman, A. Syed, A. Mawer, Microelectron. Reliab. **40**, 1117 (2000)
5. R. Ghaffarian, N.P. Kim, Microelectron. Reliab. **39**, 107 (1999)
6. X. Liu, S. Xu, G.Q. Lu, D.A. Dillard, Microelectron. Reliab. **42**, 1883 (2002)
7. D.T. Rooney, N.T. Castello, M. Cibulsky, D. Abbott, D. Xie, Microelectron. Reliab. **44**, 275 (2004)
8. Y. He, Thermochimica. Acta. **376**, 101 (2001)
9. Y. Sawada, K. Harada, H. Fujioka, Microelectron. Reliab. **43**, 465 (2003)
10. L. Leicht, A. Skipor, Microelectron. Reliab. **40**, 1129 (2000)
11. Y.S. Lai, T.H. Wang, H.H. Tsai, M.H.R. Jen, Microelectron. Reliab. **47**, 111 (2007)
12. S.C. Hung, P.J. Zheng, S.H. Ho, S.C. Lee, H.N. Chen, J.D. Wu, Microelectron. Reliab. **41**, 677 (2001)
13. J.H. Okura, S. Shetty, B. Ramakrishnan, A. Dasgupta, J.F.J.M. Caers, T. Reinikainen, Microelectron. Reliab. **40**, 1173 (2000)
14. K. Mishiro, S. Ishikawa, M. Abe, T. Kumai, Y. Higashiguchi, K.I. Tsubone, Microelectron. Reliab. **42**, 77 (2002)